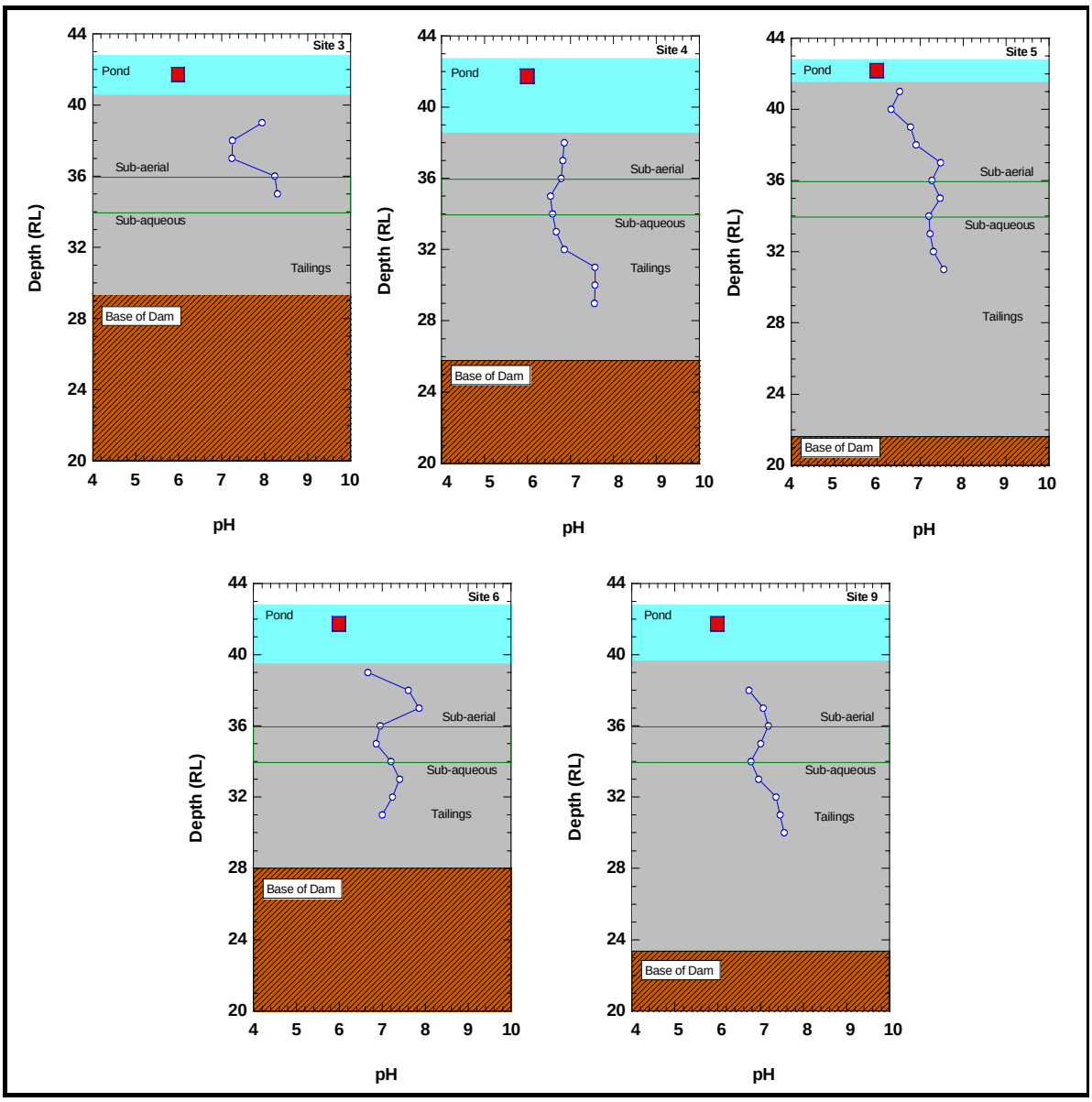

Figure 5.34: Porewater pH profiles (all stations)

The total concentrations of magnesium and sulfate in these porewaters are of the order of 0.4 M. This is equivalent to around 100 g of epsomite ($MgSO_4 \cdot 7H_2O$) per litre, which by comparison with the reported solubility of 710 g/L (Weast, 1990) shows the porewaters are still considerably undersaturated with respect to epsomite. Such trends are of concern as in the absence of appropriate controls or *in-situ* geochemical removal processes (such as ion exchange, precipitation or reduction), magnesium and sulfate may behave conservatively and leach from the tailings repository at concentrations in excess of their respective receiving water criterion. In this context, and under the Uranium Mining Environmental Control Act (1982), the maximum allowable additions to receiving waters for Mg and SO_4 are 10 and 19 mg/L, respectively.

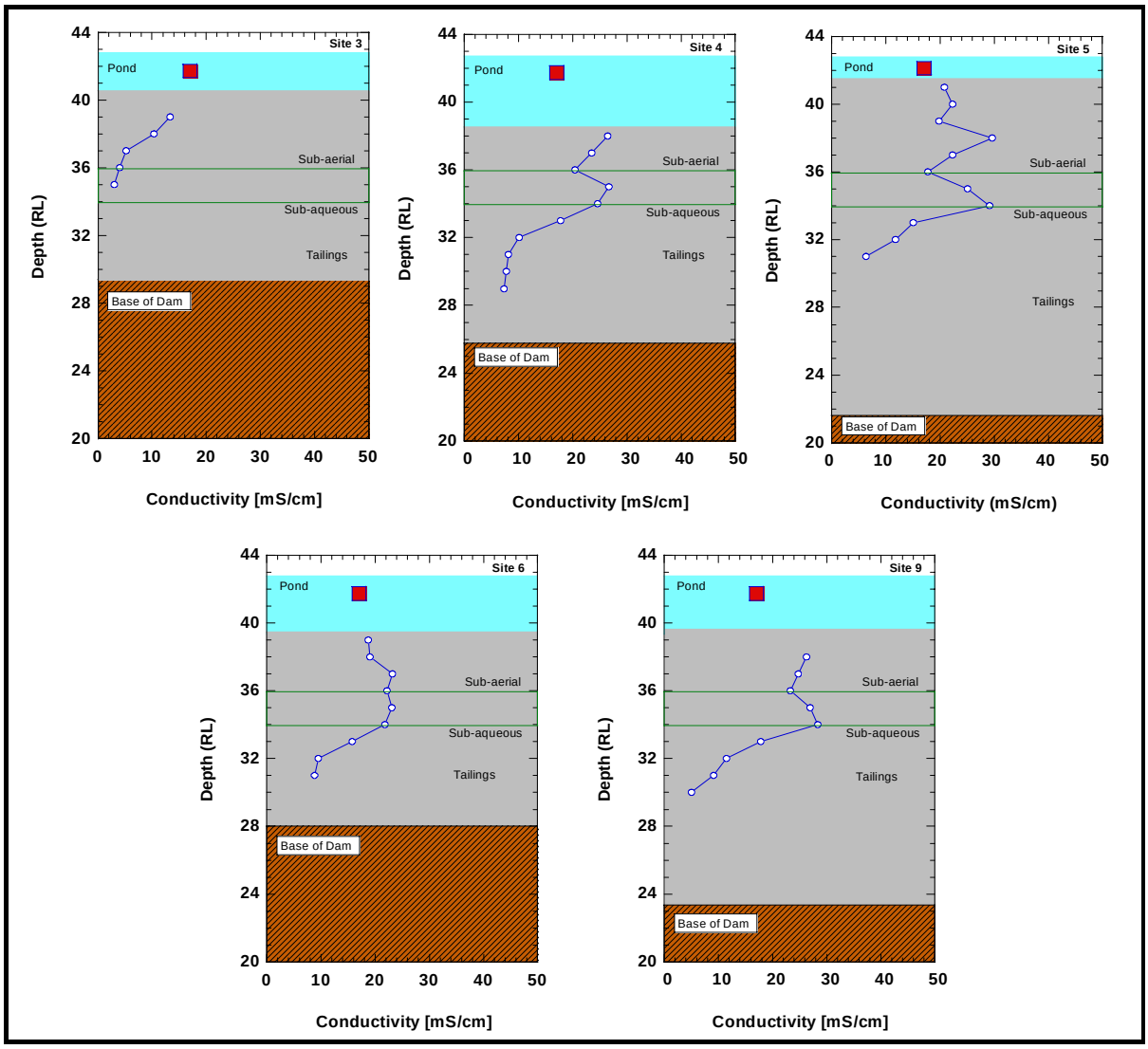

Figure 5.35: Porewater electrical conductivity profiles (all stations)

Dissolved calcium concentrations are relatively uniform over the depth profile (Figure 5.38), ranging between 400 and 500 mg/L. This trend in conjunction with the abundance of authigenic gypsum (up to 14%, see Figure 5.5) in the tailings solids suggests that calcium solubility is controlled by this mineral phase. Geochemical modelling of the porewater system using the truncated Davis equation to correct activity coefficients also confirms the observed trends with a gypsum saturation limit leading to predicted calcium concentrations of around 400 mg/L. Manganese concentrations in near surface porewaters (Figure 5.39) remain elevated (up to ~1400 mg/L) indicating that the Eh-pH relationships are not altered sufficiently by the addition of lime to cause complete precipitation of manganese oxyhydroxides. Over the depth profile, Mn behaves similarly to other major ions (Mg and SO_4), reaching a concentration maximum (700 to 1000 mg/L) at around RL 35, followed by a sharp decrease to < 50 mg/L at lower depths.

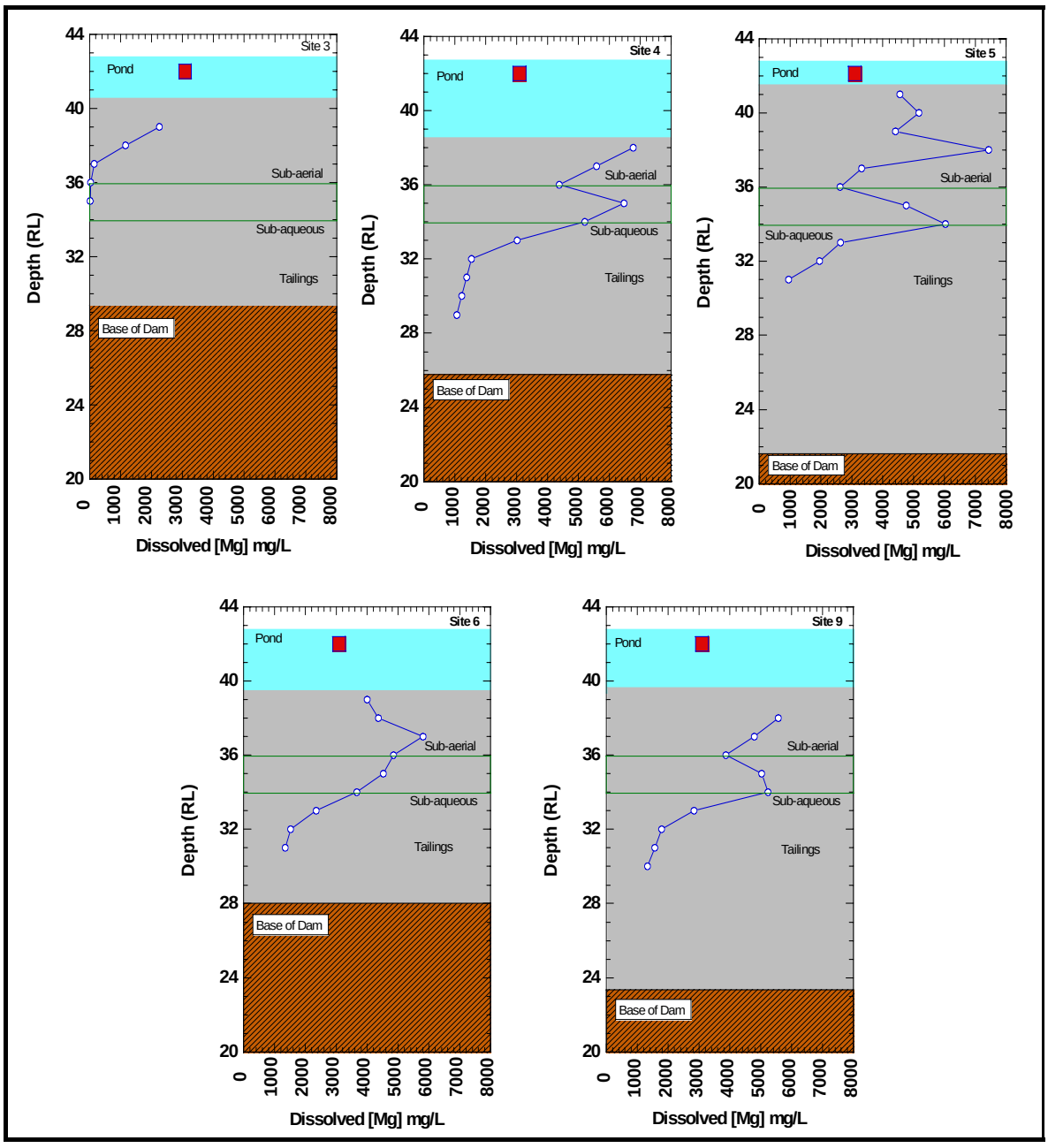

Figure 5.36: Porewater magnesium profiles (all stations)

Given the very high dissolved concentrations of Mn in the upper zone it is difficult to delineate the mechanisms (evapoconcentration/reductive dissolution) responsible for the observed trends. This combined with variable pH down the profile and two distinctive geochemical phases will make the evaluation of a realistic solubility control problematical. In addition, sub-crystalline to crystalline manganese oxides are present (see Figure 5.7) in both the upper and lower zones, which suggests that reductive dissolution may not be a primary control mechanism. In the lower zone, the abundance of these phases ranged from 0.7% to 1.2%.

Figure 5.40 shows a typical SEM field view of a MnO_x phase observed at Site 4 (11 m), which is equivalent to RL 32.

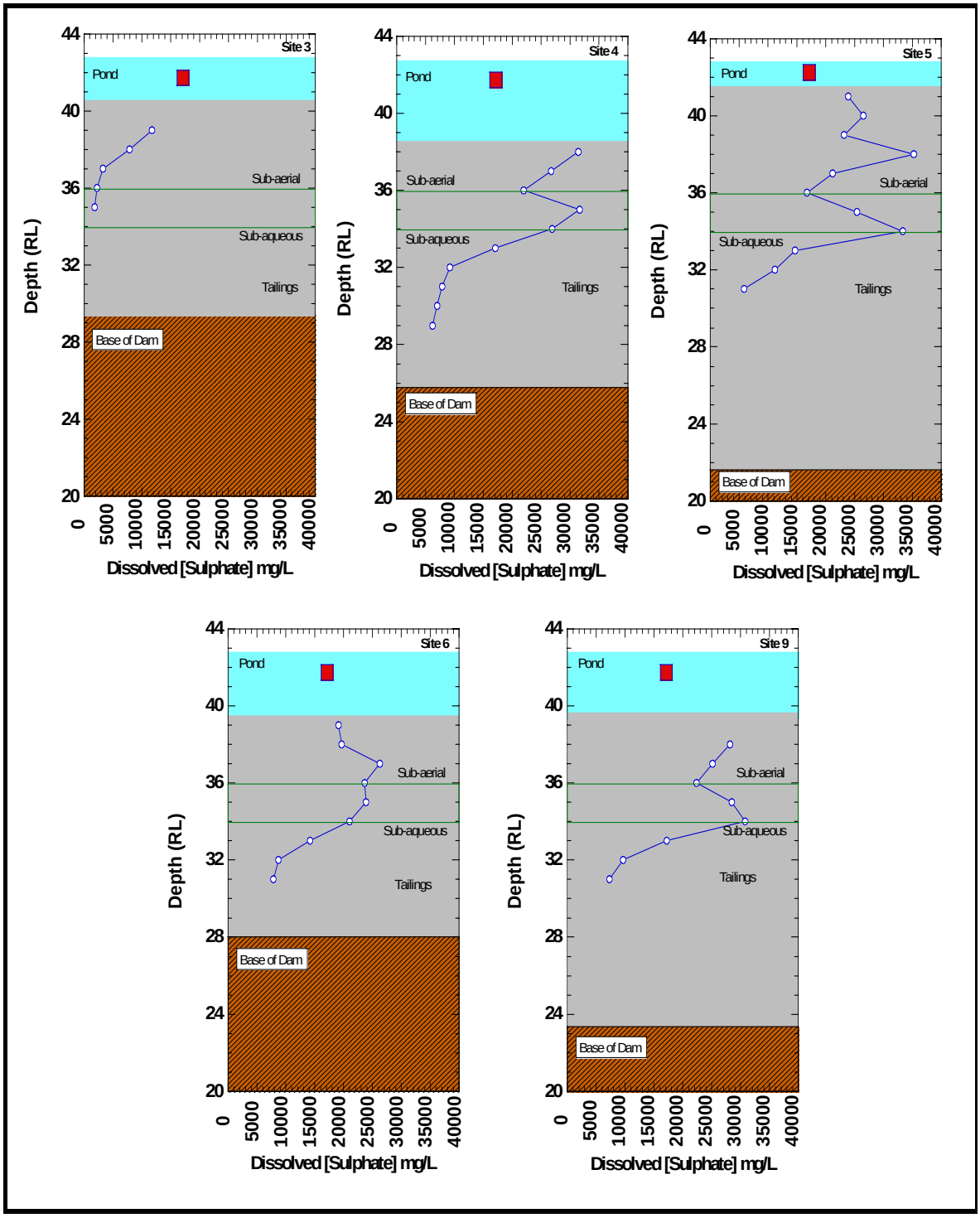

Figure 5.37: Porewater sulfate profiles (all stations)

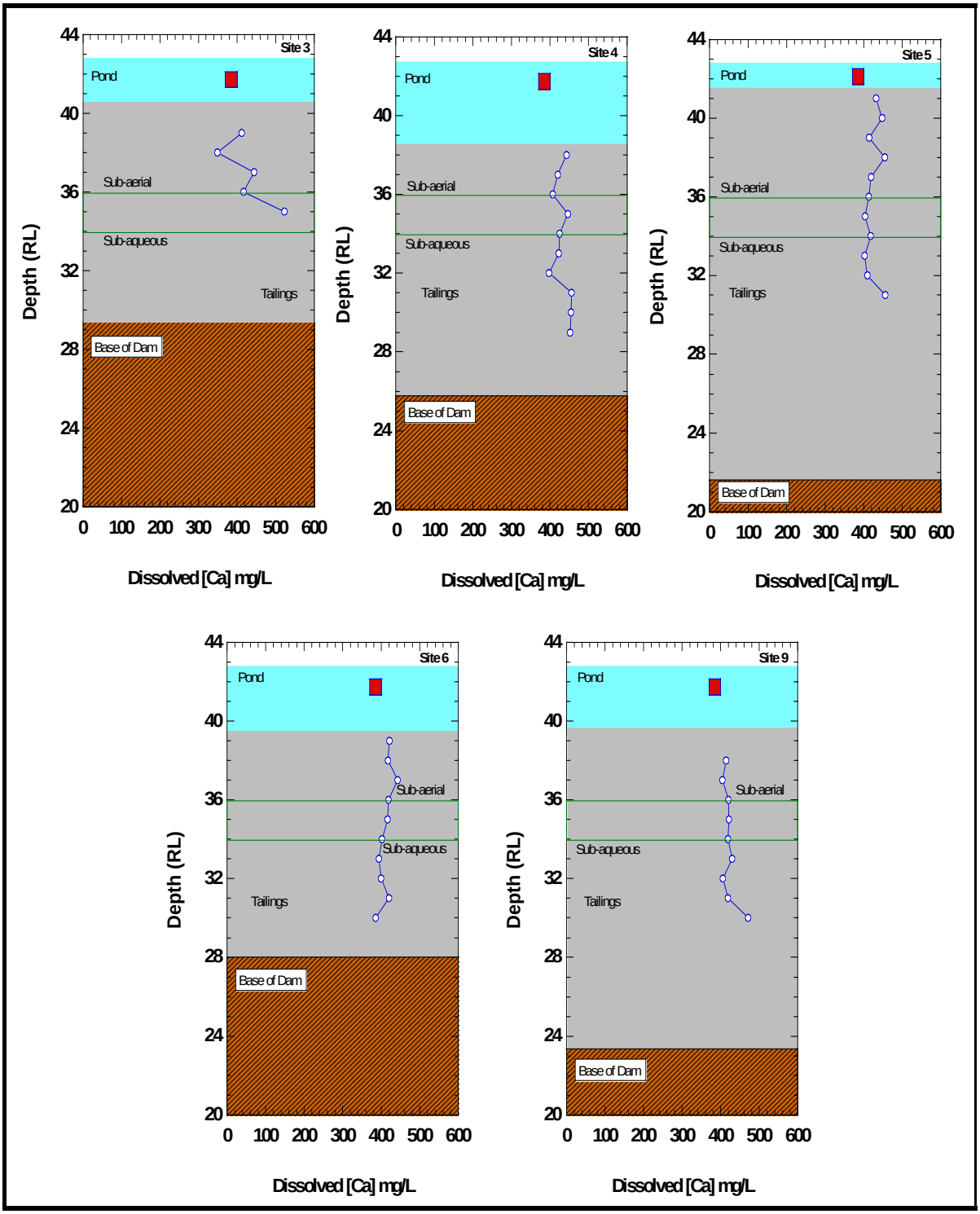

Figure 5.38: Porewater calcium profiles (all stations)

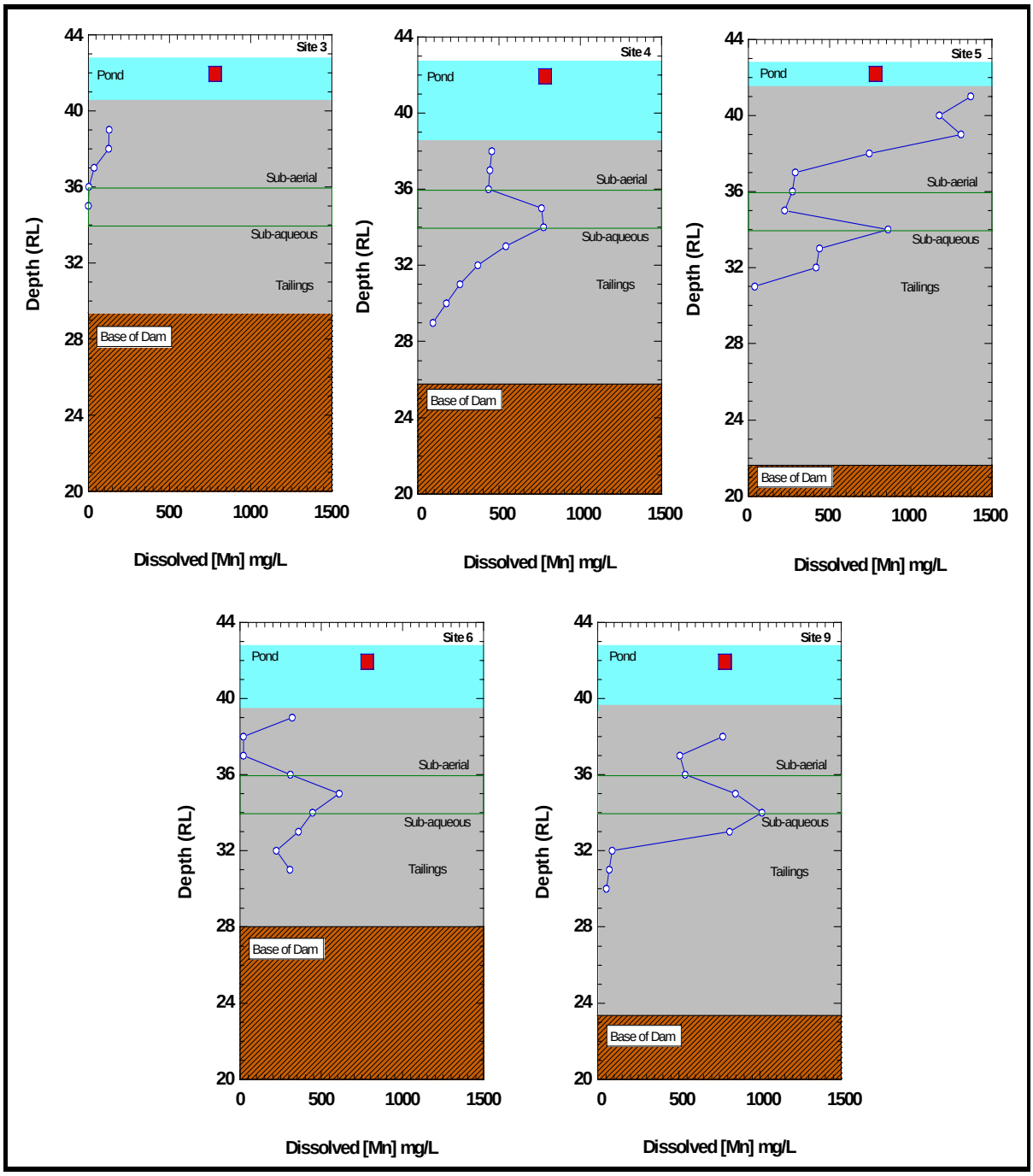

Figure 5.39: Porewater manganese profiles (all stations)

Studies by Hem (1978) and Eary (1999) show that Mn precipitation from SO_4 solutions under alkaline conditions form secondary minerals such as manganite (MnOOH) or hausmannite (Mn_3O_4). After ageing, these initial precipitates convert to a composition that approximates birnessite (γ-MnO_2). The results of this study generally concur with the findings of Hem (1978) and Eary (1999).

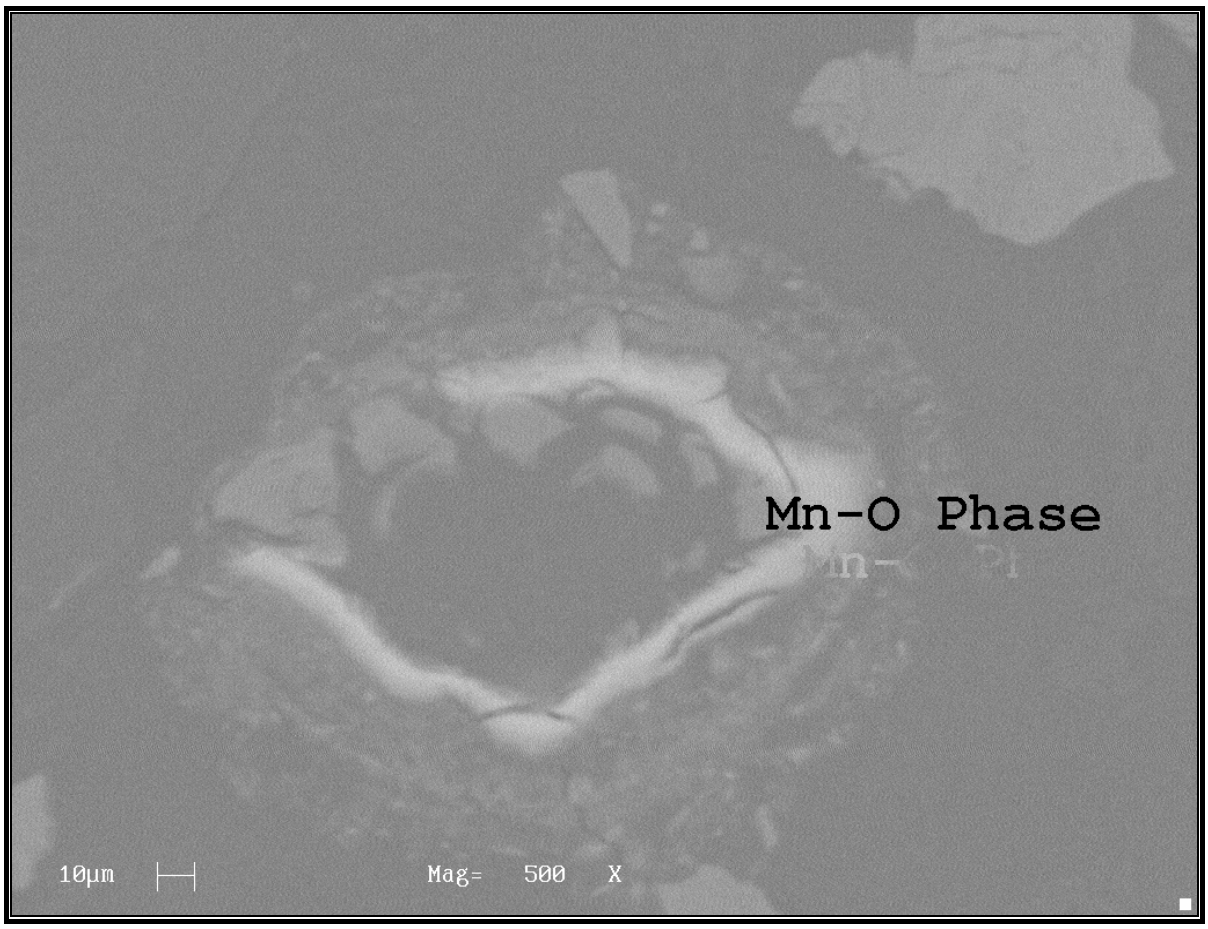

Figure 5.40: SEM field view of a MnO_x phase sampled at Site 5 (11.1 m) or RL 32

In summary, the results of this study and those by Hem (1978) and Eary (1999) imply that birnessite may be the most representative control for Mn in the tailings solids – porewater system. This phase, in addition to the formation of rhodochrosite, is further examined in Chapters 6 and 7.

Ammonium concentration profiles (Figure 5.41) are consistent with the trends exhibited by the other major ions, suggesting conservative behaviour under the prevailing geochemical environment. Concentration maxima of around 600 to 700 mg/L were typically observed in the upper zone, which is consistent with pond water levels. Below RL 35, the porewater concentrations abruptly decrease to around 100 mg/L.

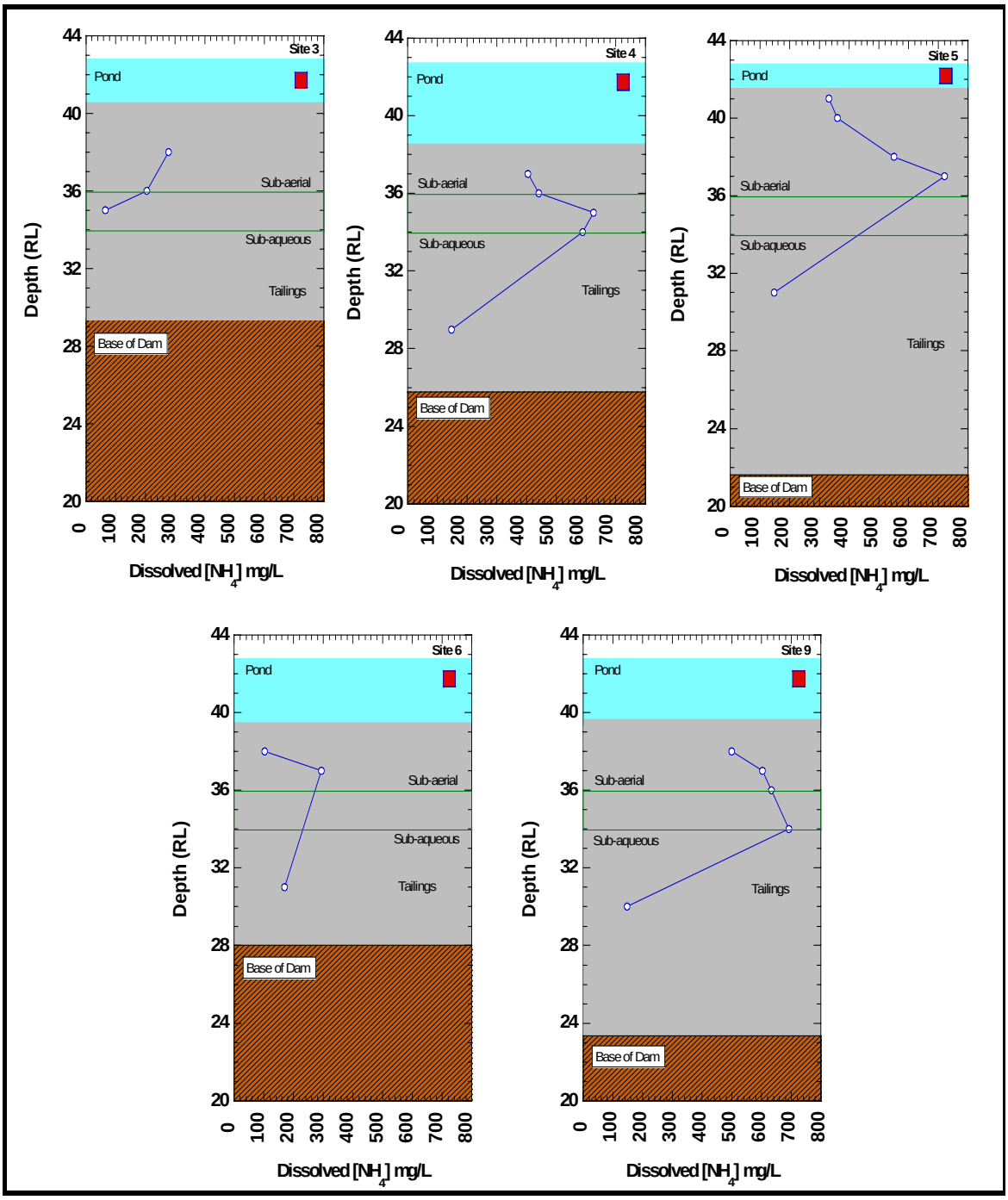

Figure 5.41: Porewater ammonium profiles (all stations)

In addition to the effects of evapoconcentration, the ammonium maxima that occurs around the sub-aerial/sub-aqueous interface may also be due to nitrate reduction that will occur as the redox potential decreases down the tailings profile:

$$0.5NO_3^- + 5H^+ + 4e^- \leftrightarrow 0.5NH_4^+ + 1.5H_2O \ (p\varepsilon = 6.15) \quad \text{.....(5.13)}$$

Below the sub-aerial/sub-aqueous interface, NH_4^+ concentrations decrease presumably as a result of higher water content (dilution) and or ion exchange with other mono cations onto clay surfaces. The redox implications of denitrification, as described in Table 5.1, are further examined in the following Section.

Like ammonia and the other major ions, the chloride porewater profiles (Figure 5.42) also confirm the distinctive transition zone between sub-aqueous and sub-aerial deposition. Chloride is known as a conservative ion (Turner and Dillon, 1988) and is thus a very good indicator of porewater enrichment/evapoconcentration that resulted from sub-aerial deposition.

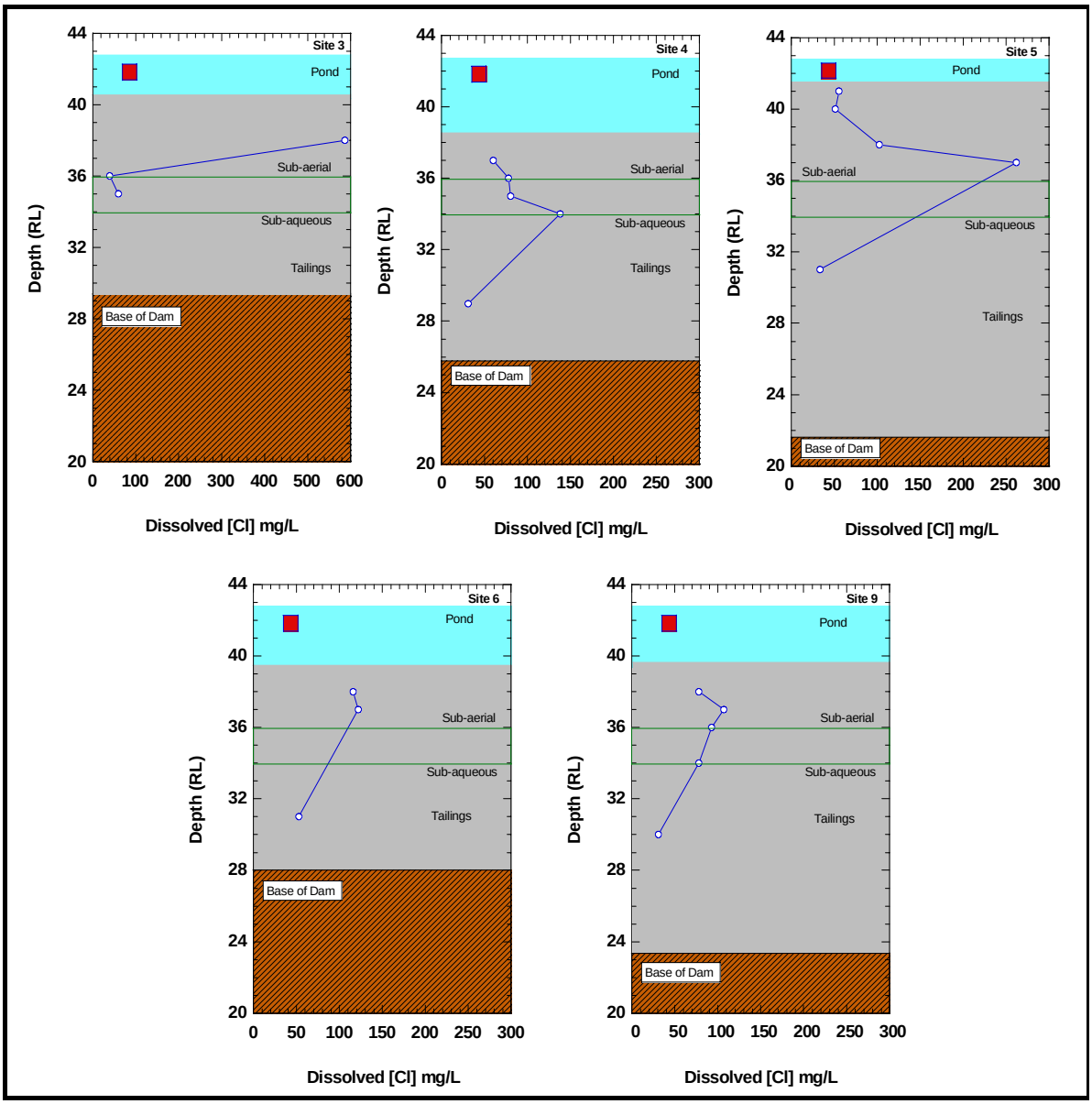

Figure 5.42: Porewater chloride profiles (all stations)

5.4.3 Porewater Redox Chemistry

As previously discussed in Section 5.1.2, the redox chemistry of tailings porewaters was assessed via examination of various redox indicators including Eh, NO_3^-, Mn, Fe and SO_4^{2-} (Figure 5.43). Site 5 was chosen to evaluate and interpret the various redox processes within the tailings pile as it represents the most complete data set Where relevant, data from other sample sites are also presented and discussed.

The Eh profile shows a slight decrease in redox potential within the uppermost 1 m of the tailings column, below which values are variable but generally increase with depth (Figure 5.43). Such data are not consistent with the current state of knowledge for permanently saturated sediments and tailings, which typically exhibit decreasing Eh with depth (McCreadie et al. 2000). Increasing Eh with depth implies the lateral or vertical advection of high Eh water from another area within the TSF. Given the unlikelihood of such an occurrence and for reasons previously outlined in Section 5.1.2, the Eh data were not used in the interpretation of porewater redox couples.

The use of sulfate as a leading redox indicator is limited as the extremely high porewater concentrations and dilution/evapoconcentration effects "swamp" any measurable trends associated with sulfate reduction. The occurrence of sulfate reduction can be inferred from vertical $\delta^{34}S$ (ratio of $^{34}S/^{32}S$) profiles. Sulfur-32 is preferentially reduced by sulfate reducing bacteria, and therefore $\delta^{34}S$ typically increases with depth over zones of sulphate reduction (McCreadie et al. 2000). Vertical profiles of $\delta^{34}S$, were not measured as part of this study however porewater samples were provided to a parallel research project in which LeGras et al. (1993) delineated sources of tailings seepage water. LeGras showed that sulfur isotope ratios down the profile were uniform indicating little to no sulfate reduction. However, further downgradient from the dam where groundwater sulfate concentrations are significantly lower, LeGras did observe reduction.

For reasons mentioned above, this technique is also inconclusive as the large mass of sulfate will easily mask a subtle increase in the isotopic ratio arising from sulfate reduction. As a consequence, other more sensitive redox indicators such as Fe were evaluated.

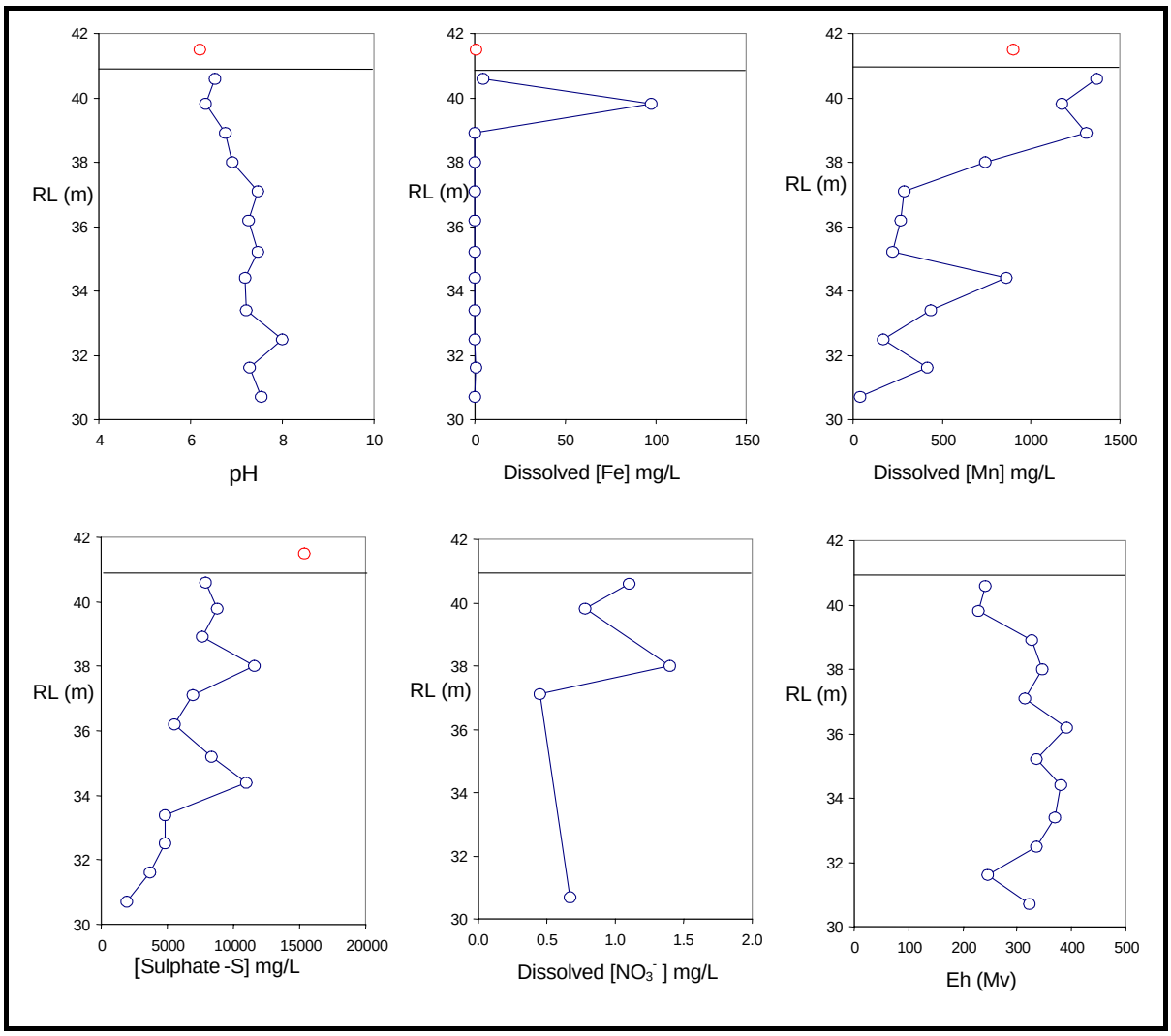

Figure 5.43: Depth distributions of pH, dissolved Fe, Mn, SO_4^{2-}, NO_3^- and Eh in porewaters at Site 5. Where available pond water concentrations are show as red circles.

Porewater iron is a well known redox indicator and within the tailings pile, dissolved concentrations increase in the near surface sediments (1 m) to ~100 mg/L (Figure 5.43). This value is considerably higher than the water column value of 0.44 mg/L, and suggests that the high porewater inventory does not stem from the overlying pond water. Rather, these data suggest that the high dissolved Fe values are derived from reductive dissolution of Fe(III) oxides. Below the zone of Fe reduction (RL 35 m), Fe is removed from solution as authigenic sulfides in accordance with the redox zonation principles described by Froelich et al. (1979). Similar results were also observed at the other sample sites as shown in Figure 5.44.

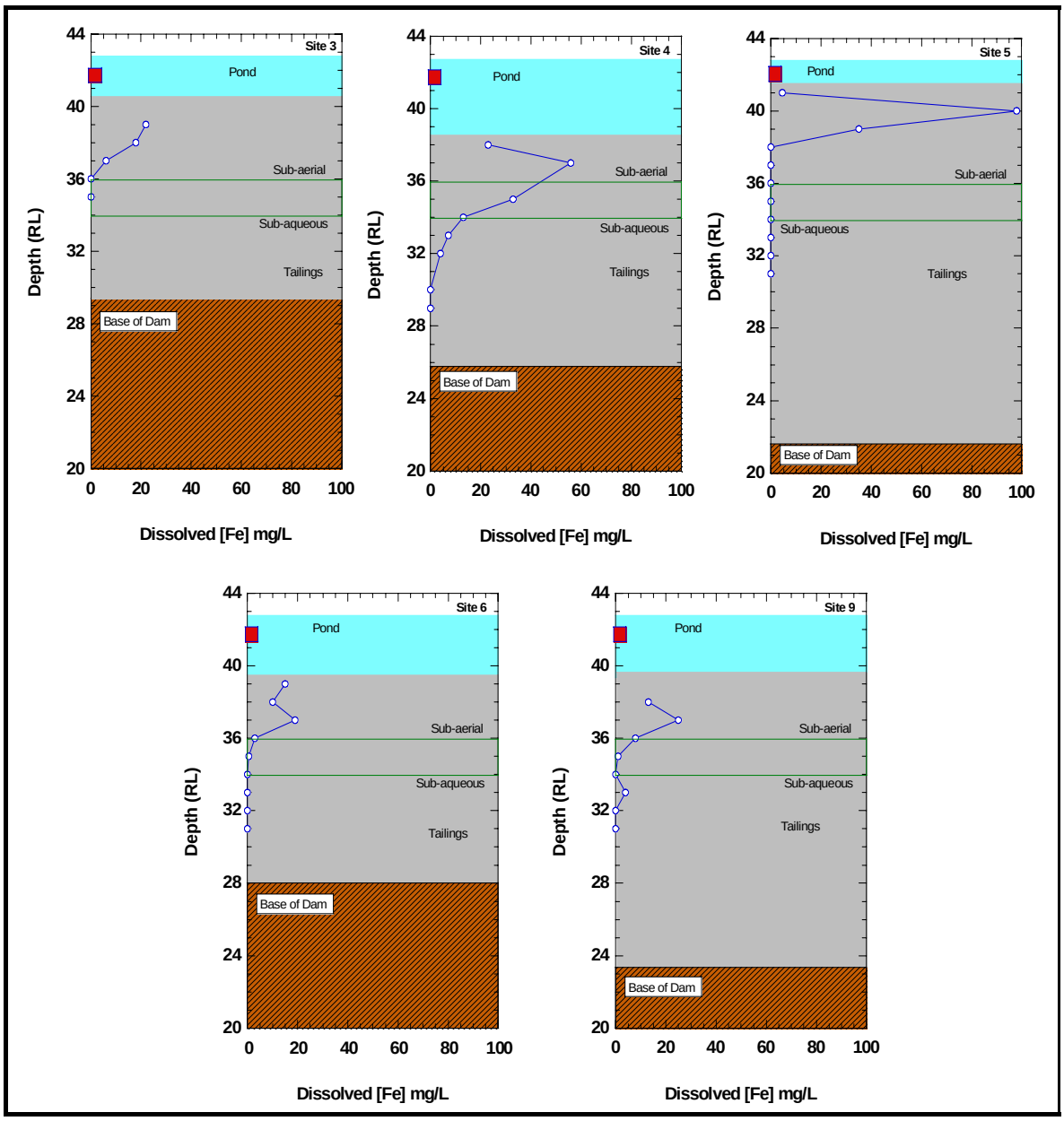

Figure 5.44: Porewater iron profiles (all stations)

Iron remobilization of this magnitude has been observed in submerged uranium mill tailings near Elliot Lake, Ontario (Martin et al. 2003) in which dissolved Fe concentrations increased from a water column value of 0.03 mg/L to 40 mg/L within the upper 10 cm of the tailings deposit.

Both the depth and magnitude of Fe remobilization are also well aligned with the solid phase abundance of readily reducible amorphous Fe oxyhydroxides (up to 23% of total available Fe) that were identified as part of the solid state speciation test work (Figures 5.23 and 5.24).

To add further support to this hypothesis, Kimber and Moen (1992) have demonstrated that the tailings in the upper profile contain concentrations of organic compounds (mainly

hydrocarbons), ranging from 2 to 21 mg/kg of wet tailings and that the tailings deposits support C-utilizing bacteria. These concentrations approximate those reported by Landa et al. (1986), in which the organic C concentrations of uranium tailings sampled at three uranium mines in the United States ranged from < 100 to 3200 mg/kg. Landa found that these concentrations were sufficient to support the microbially mediated decomposition of organic matter.

Such data imply that bacterial respiration of organic matter (OM) is occurring within the Ranger tailings pile. The sediment-oxygen demand associated with OM oxidation will result in progressively more reducing conditions with depth below the tailings-water interface, leading to the reductive dissolution of labile Fe(III) oxyhydroxides.

Dissolved Mn values (Figure 5.39) in the upper porewaters are only slightly elevated in comparison to the dam water value. Therefore, it is not clear if the dissolved Mn porewater enrichment represents a diagenetic signature or merely the influence of the water cover composition. However, given that Mn(IV) reduction is predicted to occur at a lower redox potential than Fe(III), it can be assumed that labile Mn(IV) solid phases are unstable in the suboxic tailings environment.

Profiles of other trace metals (Co, Ni, Cu and Mo) which form insoluble metal sulfide minerals were also examined (Figures 5.45, 5.46, 5.47 and 5.48). The profiles of Co and Ni mirror the Fe profile and are consistent with the notion of sulfide formation below RL 37 m. Below this RL, the concentrations of Ni and Co decrease by an order of magnitude compared with their concentrations of > 100 µg/L in the upper oxic zone. The dissolved Cu distribution does not follow the same pattern. However, elevated levels of dissolved Cu can persist in sulfidic porewaters due to the formation of strong Cu-organic or polysulfide complexes which can maintain Cu in solution.

Molybdenum like Fe, Mn and U is also known to undergo changes in oxidation state under different redox conditions. Molybdenum may occupy many oxidation states ranging from 0 to +6; however, thermodynamic data suggest it should have oxidation states of VI in oxic water and IV in anoxic environments (Stumm and Morgan, 1981). Other studies (Shimmield and Price, 1986) show that in oxic environments similar to the upper zone of the tailings pile, Mo will preferentially adsorb onto Fe and Mn oxides.

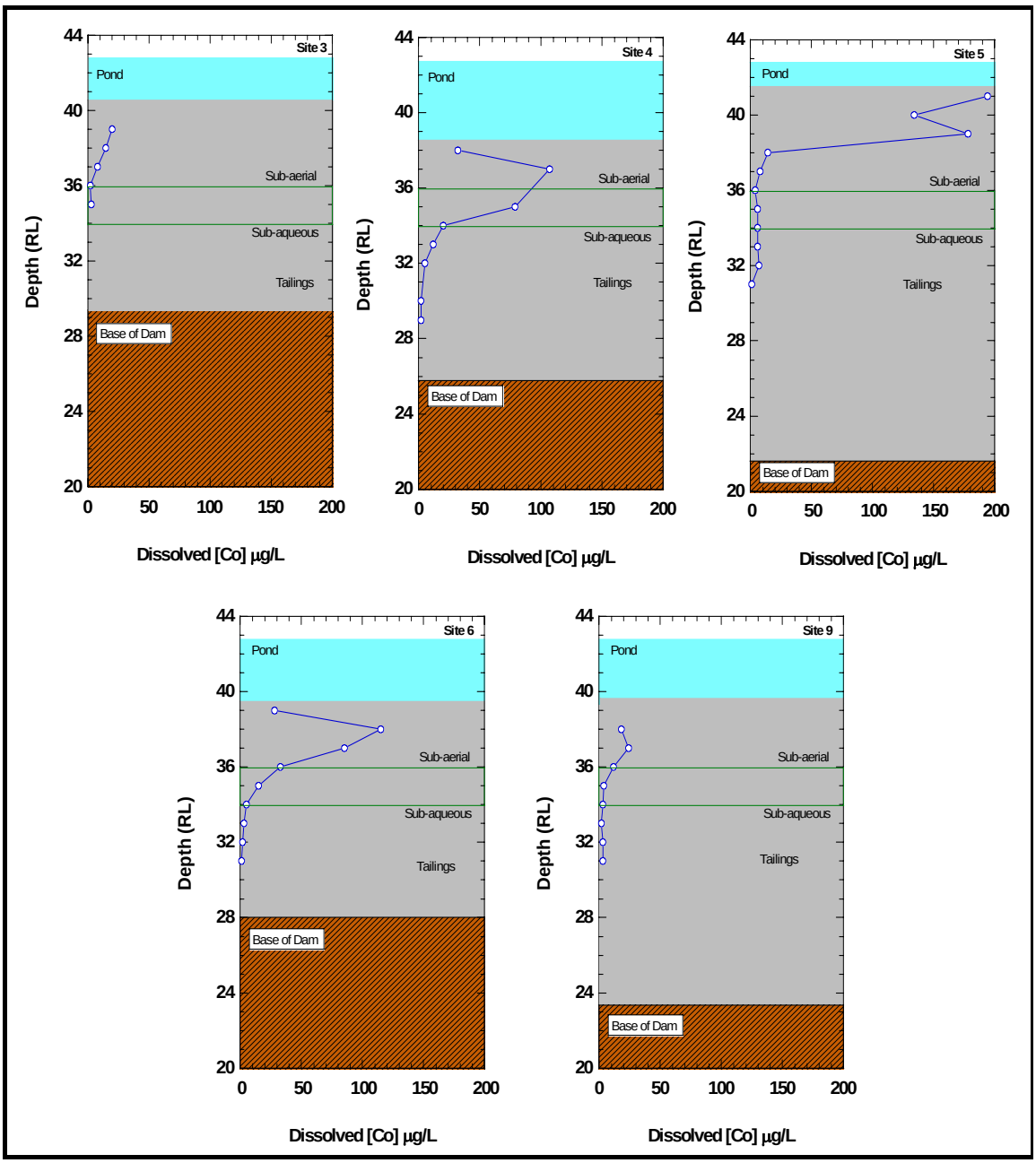

Figure 5.45: Porewater cobalt profiles (all stations) – Pond water data were not available at the time of sampling

On this basis, reductive dissolution of Fe and Mn hydrous oxide phases at or around RL 36 could account for the remobilisation of Mo. Once mobilised, Mo can either diffuse upward to be readsorbed in the more oxic Mn precipitation zone (above RL 36) or migrate downward to be fixed by sulfides. Under conditions of low redox potential, Mo is believed to be reduced to the tetravalent state and then coprecipitated with mackinawite ($FeS_{0.9}$) (Bertine, 1972). Direct precipitation as MoS_2 or MoS_3 is also a possibility but not thermodynamically favoured. The correlation between Mo removal and the formation of mackinawite is further discussed in Chapter 6.

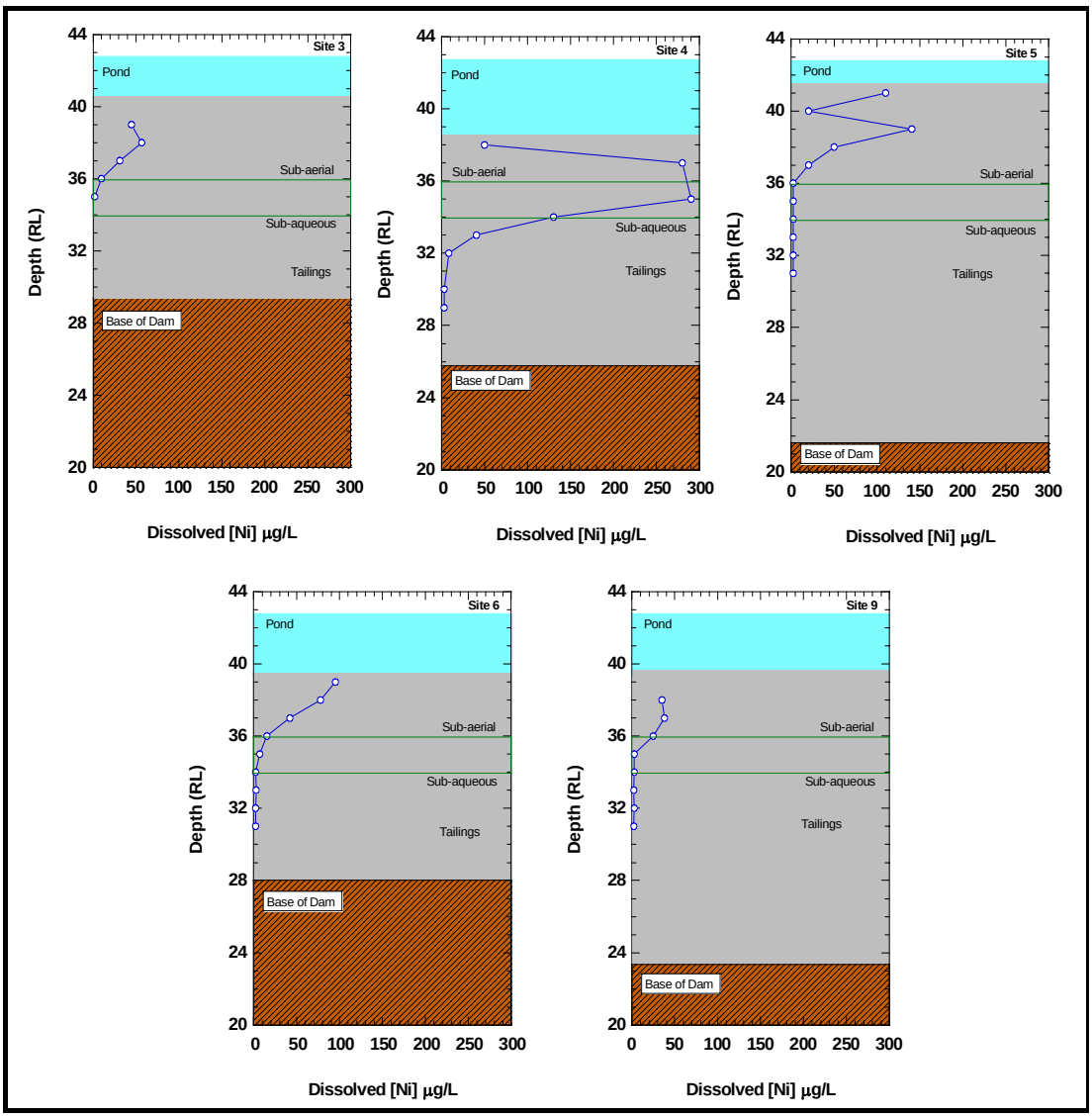

Figure 5.46: Porewater nickel profiles (all stations) – Pond water data were not available at the time of sampling

The presence of suboxic conditions as inferred from the Fe and trace metal profiles is also supported by the available pH and nitrate data. More specifically, both nitrate reduction and sulfate reduction liberate alkalinity via the oxidation of organic matter as described in Table 5.1. Accordingly, pH profiles should increase with depth as alkalinity is liberated and added to porewaters. Porewater pH profiles (Figure 5.34) are consistent with this explanation in addition to being at least one to two pH units higher than pond water pH values (Figure 5.29). This tenet provides further evidence of diagenetic processes. The data used to confirm the presence of nitrate reduction were largely drawn from previous studies conducted by Kimber and Moen (1992). Nitrate data collected as part of the present study were of limited utility because the spatial sampling resolution was not sufficient to identify near surface reduction processes.

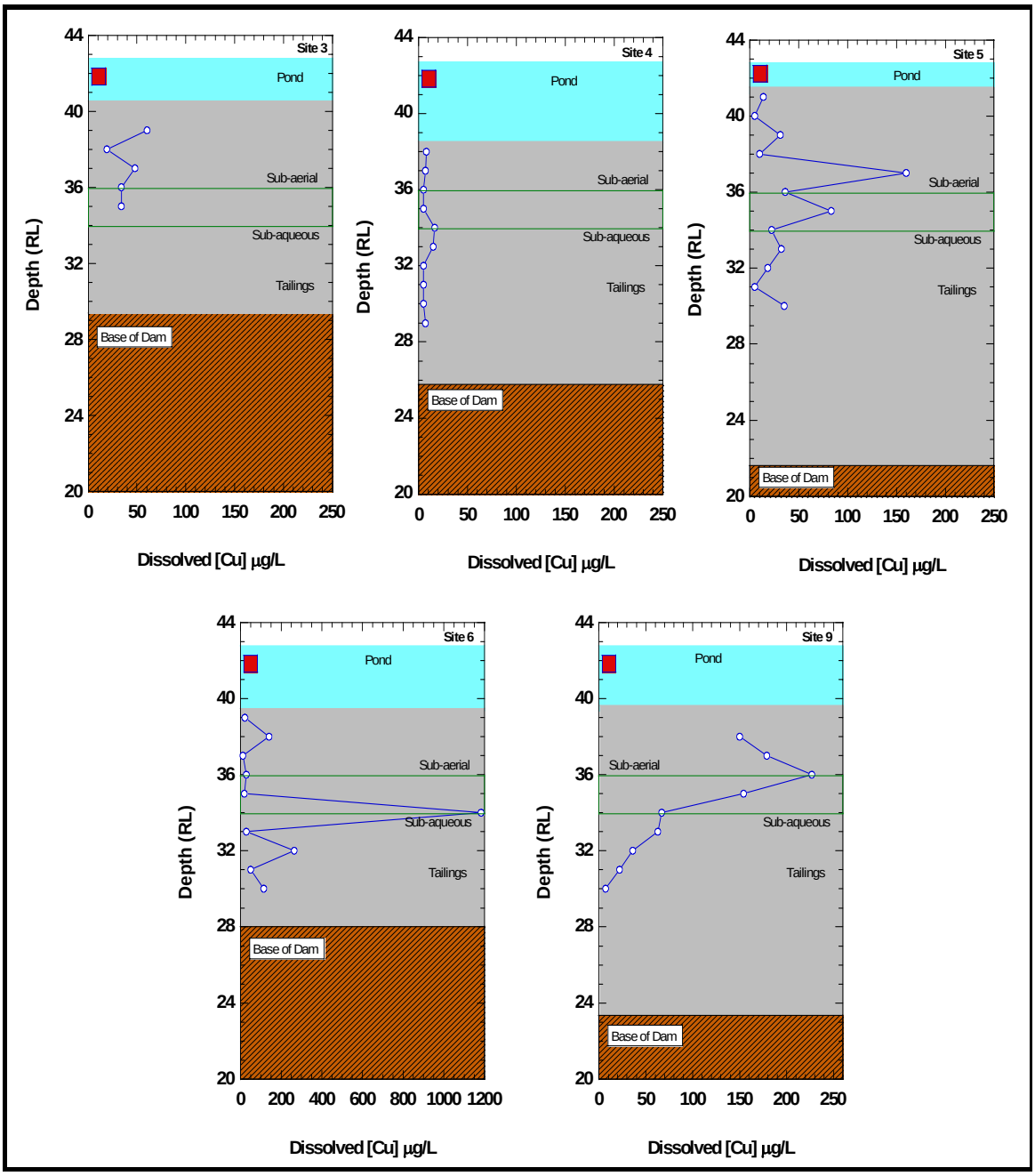

Figure 5.47: Porewater copper profiles (all stations)

Comparison of porewater nitrate profiles for this study and those of Kimber and Moen (1992) are shown in Figure 5.49. The latter data were collected in close proximity to the Site 5 of this study; hence, they are directly comparable. As shown by Kimber and Moen (Figure 5.50), porewater nitrate levels immediately beneath the tailings – pond water interface rapidly decrease from 66 mg/L at a depth of 0.2 m to levels near the detection limit (0.5 mg/L) at a tailings depth of 2 m (Figure 5.50). In contrast, the sample resolution, as highlighted by the Site 5 was not sufficient to identify this very important geochemical trend. As a consequence, these data were excluded from the present study.

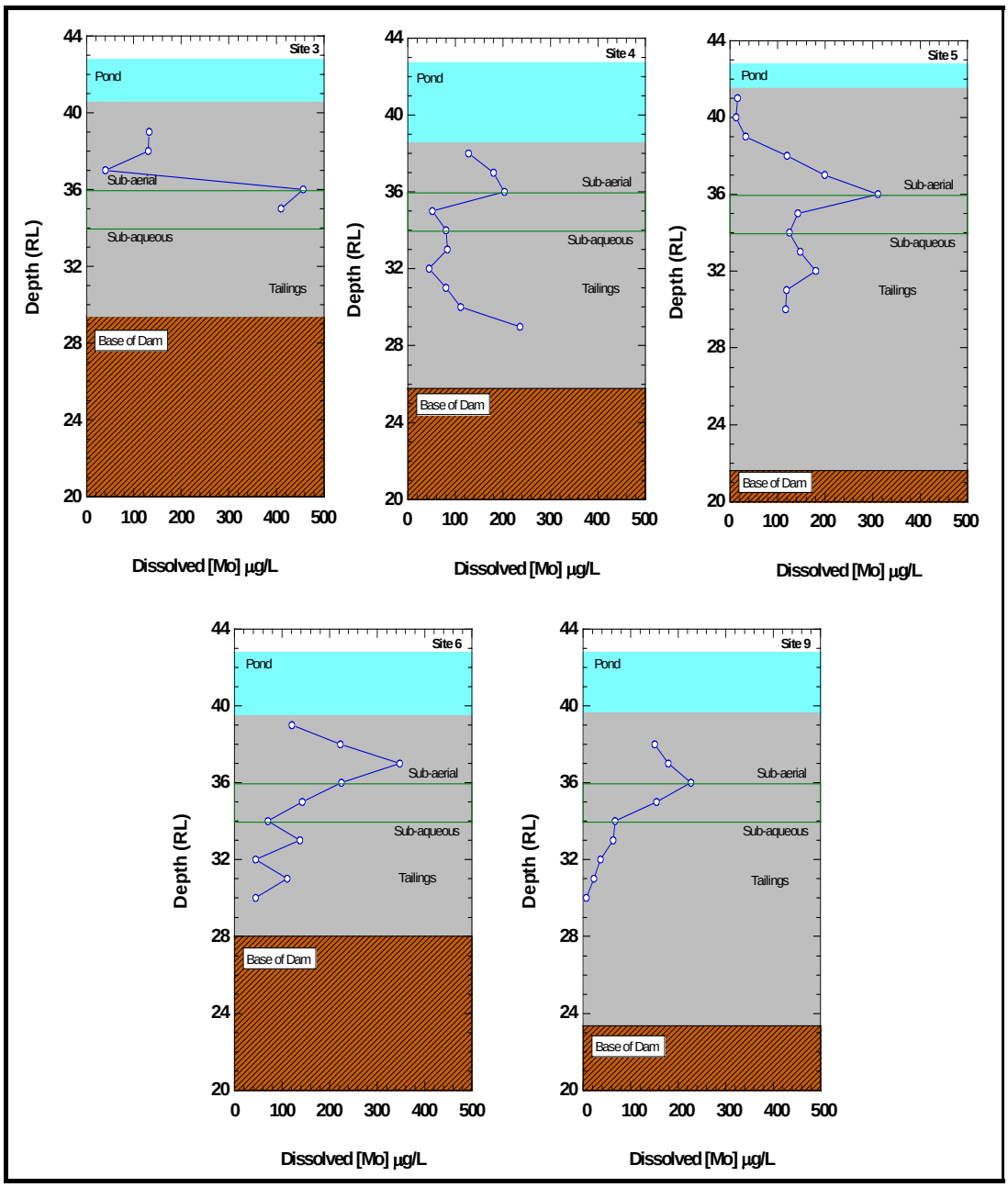

Figure 5.48: Porewater molybdenum profiles (all stations) – Pond data were not available at the time of sampling

Aligning these field observations with the geochemical theory outlined in Section 5.1.2, suggests that in the absence of oxygen, nitrate represents the preferred electron acceptor in the oxidation of organic matter. In this thermodynamic scheme (see Table 5.1), redox reactions involving nitrate reduction should occur prior to Fe(III) reduction. As shown in Figure 5.44, iron remobilization appears to occur at deeper depths than nitrate reduction (Figure 5.49), and suggests that their respective distributions are consistent with established redox zonation principles (Froelich et al. 1979).

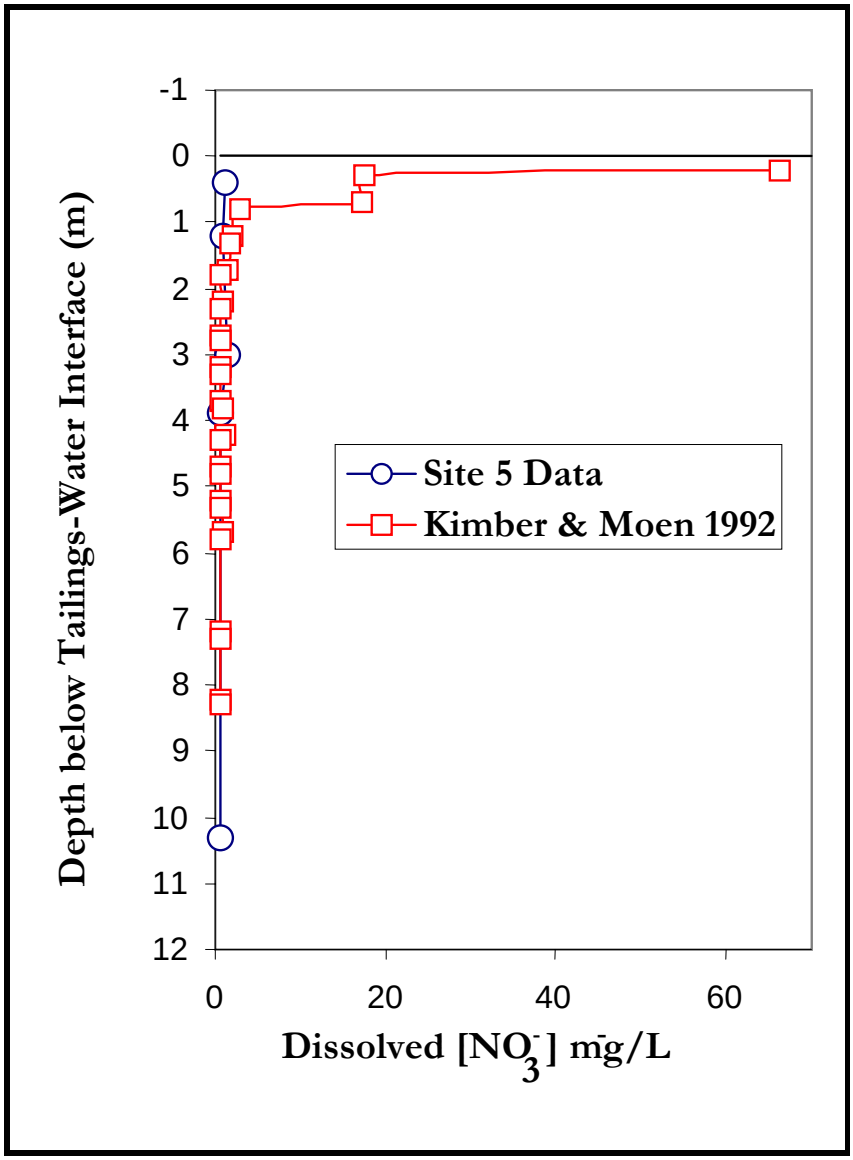

Figure 5.49: Depth distributions of dissolved NO_3^- in tailings porewaters, comparison of Ranger data (Site 5) and those of Kimber and Moen (1992).

Collectively, the nitrate, pH, Fe and trace metal data imply that suboxic conditions occur within close proximity (< 0.5 m) to the tailings-water interface. These data are consistent with other permanently saturated and submerged tailings deposits, in which the oxidation of organic matter results in the development of suboxic conditions in the near-surface horizons (Pedersen et al. 1993; Martin et al. 2001; Vigneault et al. 2001; Martin et al. 2003).

5.4.4 Uranium and Radium Mobility

5.4.4.1 Factors Governing Mobility

The behaviour of uranium in aqueous systems is strongly dependent on redox conditions. The reduction of U(VI) to U(IV) can occur in reducing environments via: 1) dissimilatory reduction involving Fe(III)-reducing micro-organisms; or 2) abioligical reactions involving sulfide, or organic compounds as the reductant (Lovely et al. 1991; Fredrickson et al. 2000). As shown in Table 5.1, the redox potential at which U(VI) is reduced to U(IV) is similar to that for the reduction of Fe(III) to Fe(II) (Langmuir, 1978). In this context, the oxidation of organic matter coupled to the sequential reduction of Fe(III) and U(VI) is an important process affecting the geochemistry of suboxic tailings.

Uranium is particle reactive, and therefore, tends to be immobilized via removal from solution onto particle surfaces. Indeed, the primary accumulation pathway for uranium in marine sediments occurs by diffusion of U(VI) across the sediment-water interface and precipitation of insoluble phases which form when U(VI) is reduced to U(IV) (Klinkhammer and Palmer, 1991). Thermodynamic calculations predict that U(IV) should predominate in reducing waters. However, observations of the persistence of U(VI) in sulfide-rich reducing environments demonstrate that the kinetics of the reaction can be slow (Anderson et al. 1989).

In acid leach tailings alkaline earth sulfate minerals such as barite ($BaSO_4$), celestine ($SrSO_4$) and gypsum ($CaSO_4 \cdot 2H_2O$) are known to co-precipitate radium (Landa et al. 1986). However, it is generally accepted that of these minerals, radium acts more like a chemical analogue of barium, and as a result, the two elements tend to cycle together in aquatic environments (Carroll et al. 1993; Moore 1997;). Concordant behaviour of Ra and Ba in uranium mill tailings (Snodgrass and Hileman, 1985) is also the basis for Ra removal from U-mill waste streams via coprecipitation with barite.

Radium-Ba associations have also been shown to dominate in leachates of uranium mill tailings (Goulden et al. 1998). Although radium is not involved directly in redox reactions, poorly crystalline and/or amorphous secondary barite can undergo reductive dissolution in anaerobic tailings deposits (Martin et al. 2003). The dissolution of such precipitates creates potential for the release of elevated radium levels to contacting waters.

As previously discussed in Section 5.3.2, other possible mechanisms governing radium solubility include adsorption onto amorphous Fe and Mn oxyhydroxides.

These studies together with the mechanisms discussed in Section 5.1 were used to evaluate and explain the nature of uranium and radium mobility in the Ranger tailings pile.

5.4.4.2 Uranium Mobility

Porewater profiles for dissolved U (Figure 5.50) are variable and as such it is difficult to draw firm conclusions from the observed trends. In general however, the U porewater profiles show a concentration minima coincident with Fe maxima (see Figure 5.44) in the near surface sediments (> RL 39 m). Below this horizon, U levels at most sites exhibit a concentration maximum (between RL 37 to 36 m) with values ranging from 180 to 800 µg/L. Within the constraints of available data, a second concentration peak is observed at RL 33 below which U levels significantly decrease (Sites 3 and 6) to around 1 µg/L.

Such observations imply either:

1) U is not appreciably associated with reducible Fe(III) oxyhydroxides in the upper horizons, or

2) U is associated with Fe(III) oxides and is redistributed following reductive dissolution of Fe in accordance with the following authigenic processes:

   - RL > 39 m; U(VI) is initially mobilised following reductive dissolution of Fe oxyhroxides but is quickly adsorbed onto other phases or precipitated as a uranyl hydroxide such as schoepite ($UO_3 \bullet 2H_2O$).

   - RL 37 to 33 m; U(VI) solid phases are solubilised as either uranyl carbonate and or sulfate complexes as described by equations in Table 5.1. These same processes are likely to occur at RL 33 m; and

   - RL < 32 m; U(VI) is reduced to U(IV) as strongly reducing ($p\varepsilon < 0.11$) conditions develop, precipitating as uraninite (UO_2).

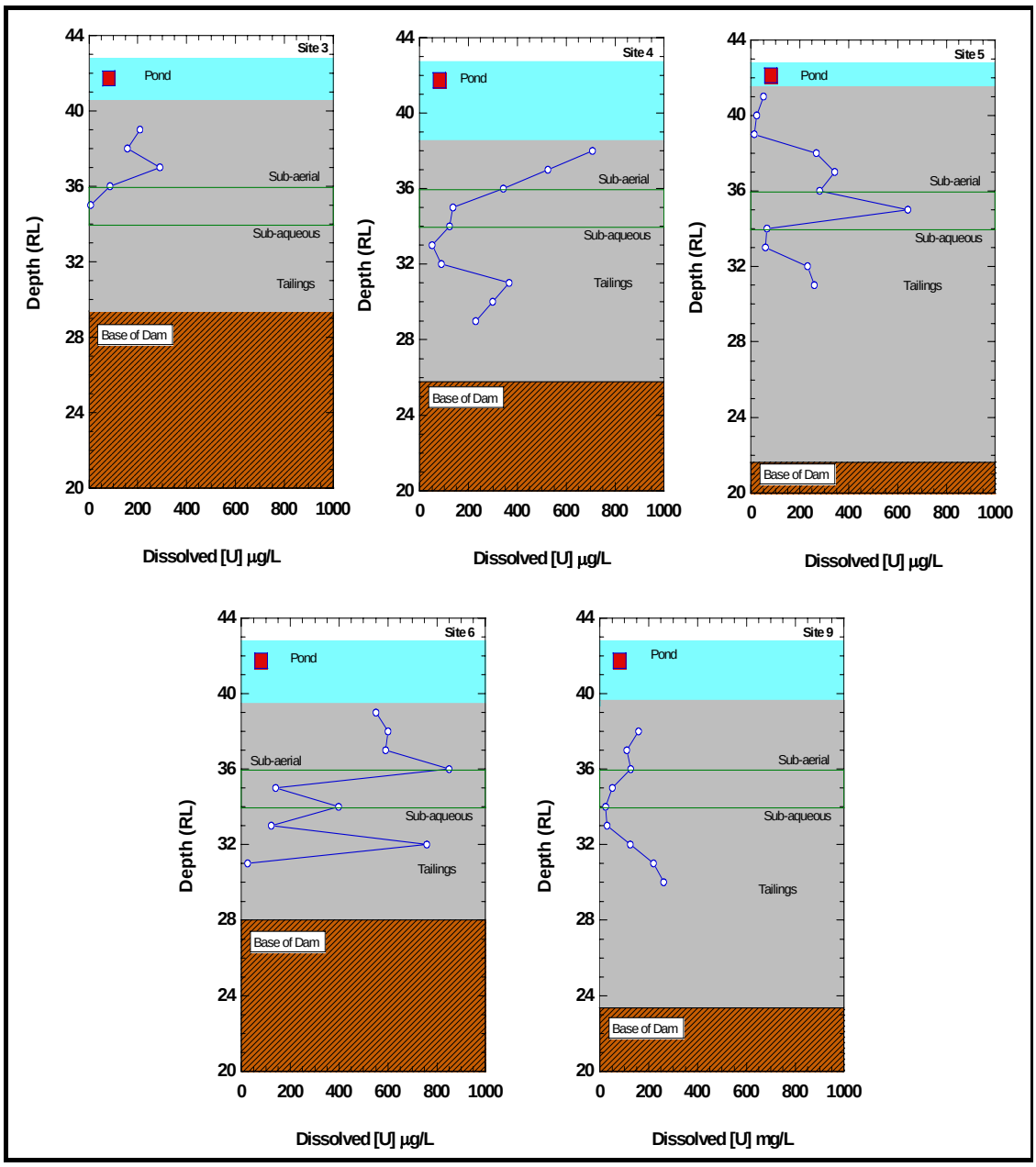

Figure 5.50: Porewater uranium profiles (all stations)

Scenario 2 is the most plausible explanation as at the time of deposition (≈1986/7) the overlying pond water U concentrations were on the order of 50 µg/L (see Figure 5.33), which is well below the observed porewater maxima of around 800 µg/L. This suggests that U is being mobilised within the tailings pile via diagenetic processes rather than being supplied from the inventory of overlying pond water. Furthermore, the results of the solid state speciation test work (Section 5.3) confirm that 35 to 40% of the total U contained in the gel and fine grain tailings is associated with readily reducible phases such as amorphous Fe oxyhydroxides. These phases act as a significant sink for labile U and given their abundance, in

both the upper sub-aerial and lower sub-aqueous horizons, it is conceivable that the redistribution of U(VI) coincident with the reductive dissolution of Fe(III) oxyhroxides is a likely hypothesis.

Within the zone of U maxima (RL 37 to 36 m), U(VI) remains the dominant form as U(IV) is largely insoluble at the neutral pH of the porewaters. At this depth it is hypothesised that uranyl hydroxide phases dissolve in the presence of increased alkalinity (arising from the oxidation of organic matter) to form stable uranyl carbonate complexes. Soluble uranyl sulfate complexes are also thermodynamically stable under the prevailing redox conditions and as such are also likely to dominate U speciation.

Below the porewater maximum, the decrease in U concentration likely reflects the reduction of U(VI) to U(IV) and the formation of insoluble uraninite in accordance with the half cell reactions described in Table 5.1.

These trends are further examined in Chapter 6 as the paucity of available porewater alkalinity data and variability of U reduction kinetics down the core profiles only permit a qualitative assessment of possible geochemical mechanisms.

The conceptual scheme presented here is however, similar to the trends observed by Cochran et al. (1986) in their study of the behaviour of U in the anoxic sediments of a marine basin. A generalised U profile derived from the Cochran study is shown is Figure 5.51 and when compared to Figure 5.50 shows the following similarities:

- U minimum close to the sediment-water interface; followed by
- Increasing concentrations to a broad maximum; and
- A decrease below the porewater maximum.

While there are similarities between the shapes of the two profiles, the rationale to account for the observed trends differs between the two studies. The Cochran study proposed a model in which the U oxidation state alternates down the profile (Figure 5.51) until the redox potential is sufficient to permanently reduce U(VI) to the more insoluble U(IV) state. The rationale for this model is not described, particularly in regard to the genesis or source of the U(VI) state at depth following the initial reduction of U(IV) in the near sediments. In contrast this study proposes a model, whereby the U(VI) oxidation state dominates the porewater profile as a

result of the formation of stable carbonate and sulfate complexes as described in Table 5.1. The carbonate is derived from the oxidation of organic matter at depth by microbial action. Such species are thermodynamically favoured at the zone of U maxima and prevail until the redox intensity falls below a pε ≈ 0.11 at which time U(VI) is reduced and precipitates as uraninite.

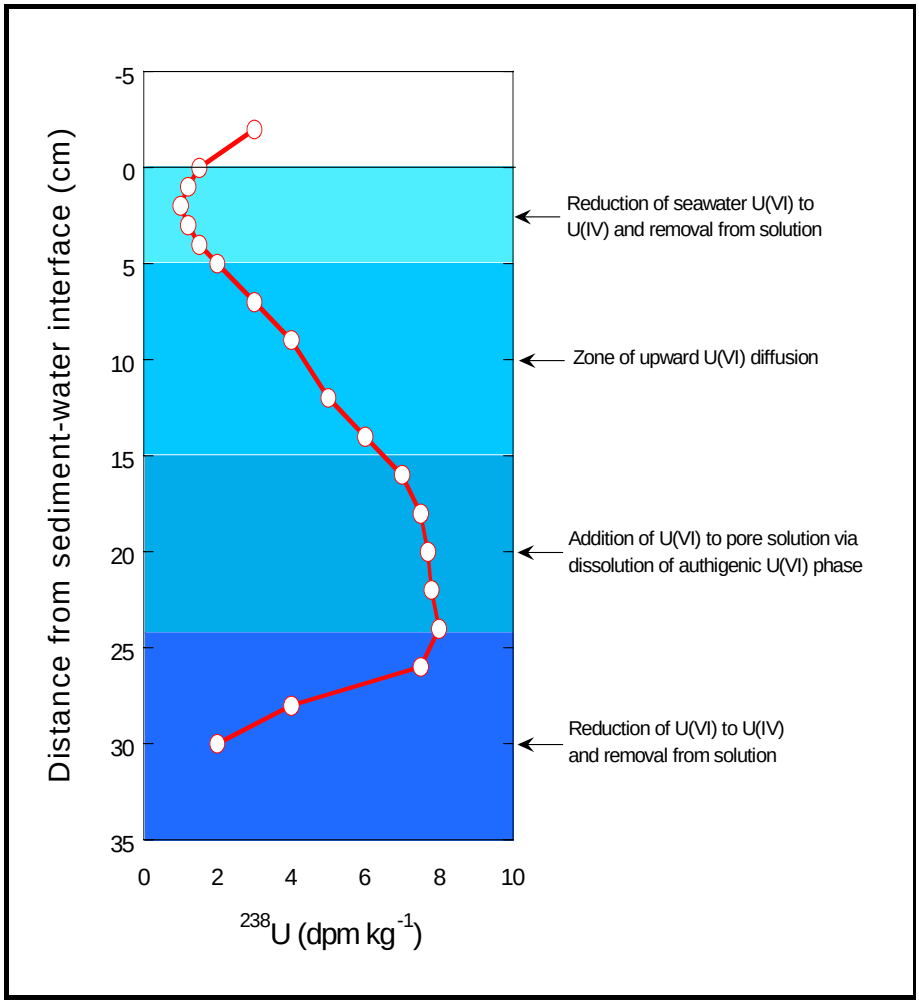

Figure 5.51: Schematic representation of data from Cochran et al. (1986) illustrating the behaviour of uranium in anoxic marine sediments

In summary, these data suggest that in the long-term, U will continue to be remobilized at mid depths via the dissolution of a U(VI) solid phase. However, the reduction of U(VI) to U(IV) and subsequent immobilization towards the base of the repository probably serves as an effective removal mechanism which limits the transfer of U to groundwaters.

Radium Mobility

As outlined above (Section 5.4.4), the behaviour of Ra in submerged uranium mill tailings can be tied to the cycling of Ba, given their similar geochemical behaviours. To elucidate the controls governing the mobility of Ra, comparisons were made between the porewater profiles of both Ba and Sr (Figures 5.52, 5.53 and 5.54). Radium activity maxima generally occur between RL 37 and 34 with levels reaching as high as 14.5 Bq/L. Outside of this zone, Ra activities decrease to < 3 Bq/L. These values are in excess of the criterion value of 0.01 Bq/L for the protection of human health (ANZECC/ARMCANZ, 2000). For this reason, knowledge of the geochemical behaviour of Ra is key to the development of appropriate design criteria for the safe closure of the tailings repository.

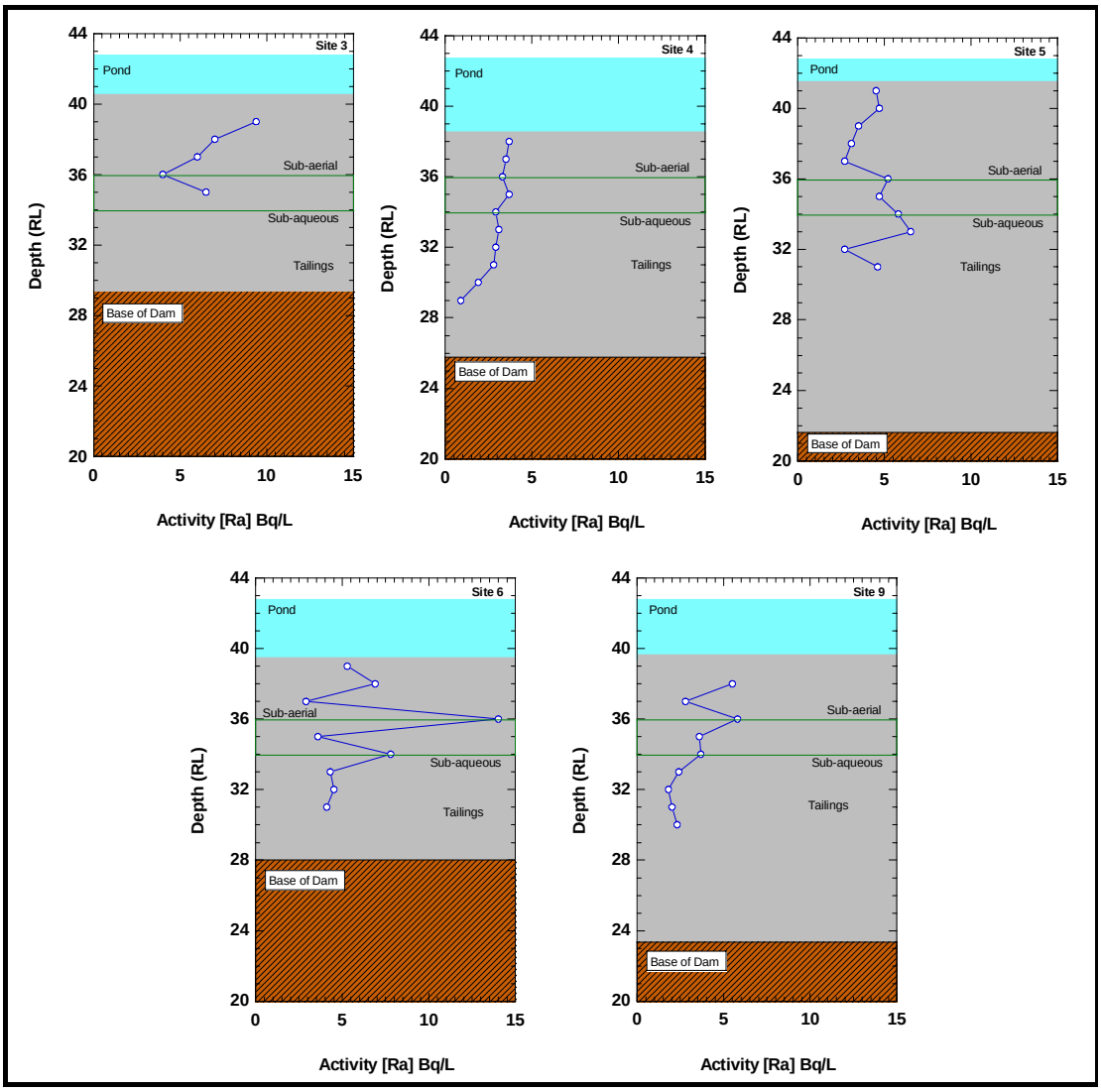

Figure 5.52: Porewater radium profiles (all stations) – Pond water data were not available at the time of sampling

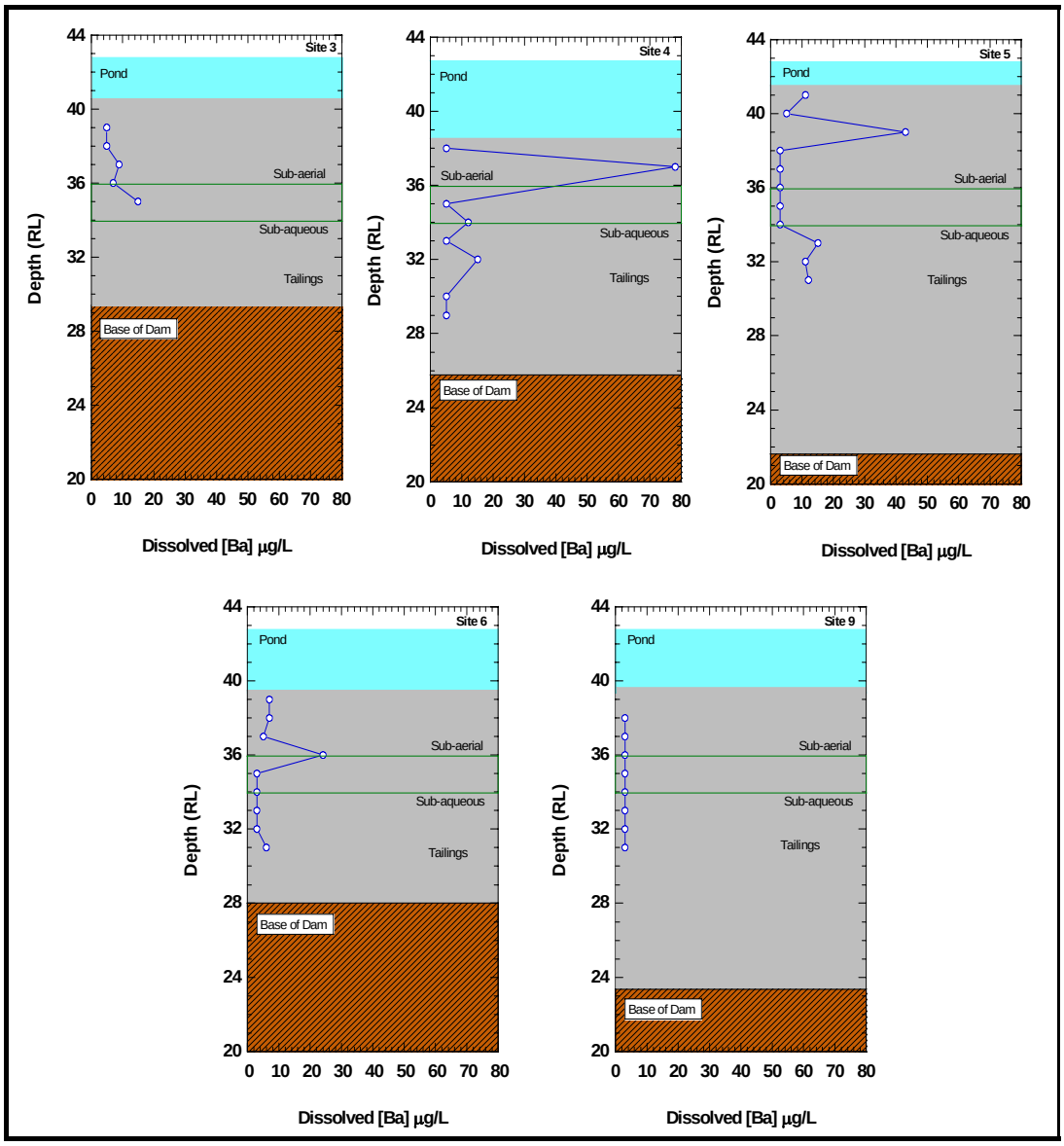

Figure 5.53: Porewater barium profiles (all stations) – Pond water data were not available at the time of sampling

Radium porewater profiles do not correlate well with either Sr or the expected geochemical analogue Ba. Such trends while inconsistent with other studies can perhaps be attributed to the presence of a non-barite host phase for Ra. Indeed, porewater concentrations of Ba are exceedingly low, with most values at or near the detection limit of 0.005 mg/L. The reductive dissolution of Ra-bearing barite or radiobarite, can result in the addition of substantial Ra to porewaters. In a uranium tailings impoundment in Canada, for example, the dissolution of radiobarite in reducing horizons resulted in elevated levels in porewaters of ≈80 Bq/L (Martin et al. 2003). The relatively low Ra and Ba values measured in the porewaters suggest that such processes are not occurring to any appreciable extent and that other mechanisms are controlling the mobility of Ra under the predicted reducing environment.

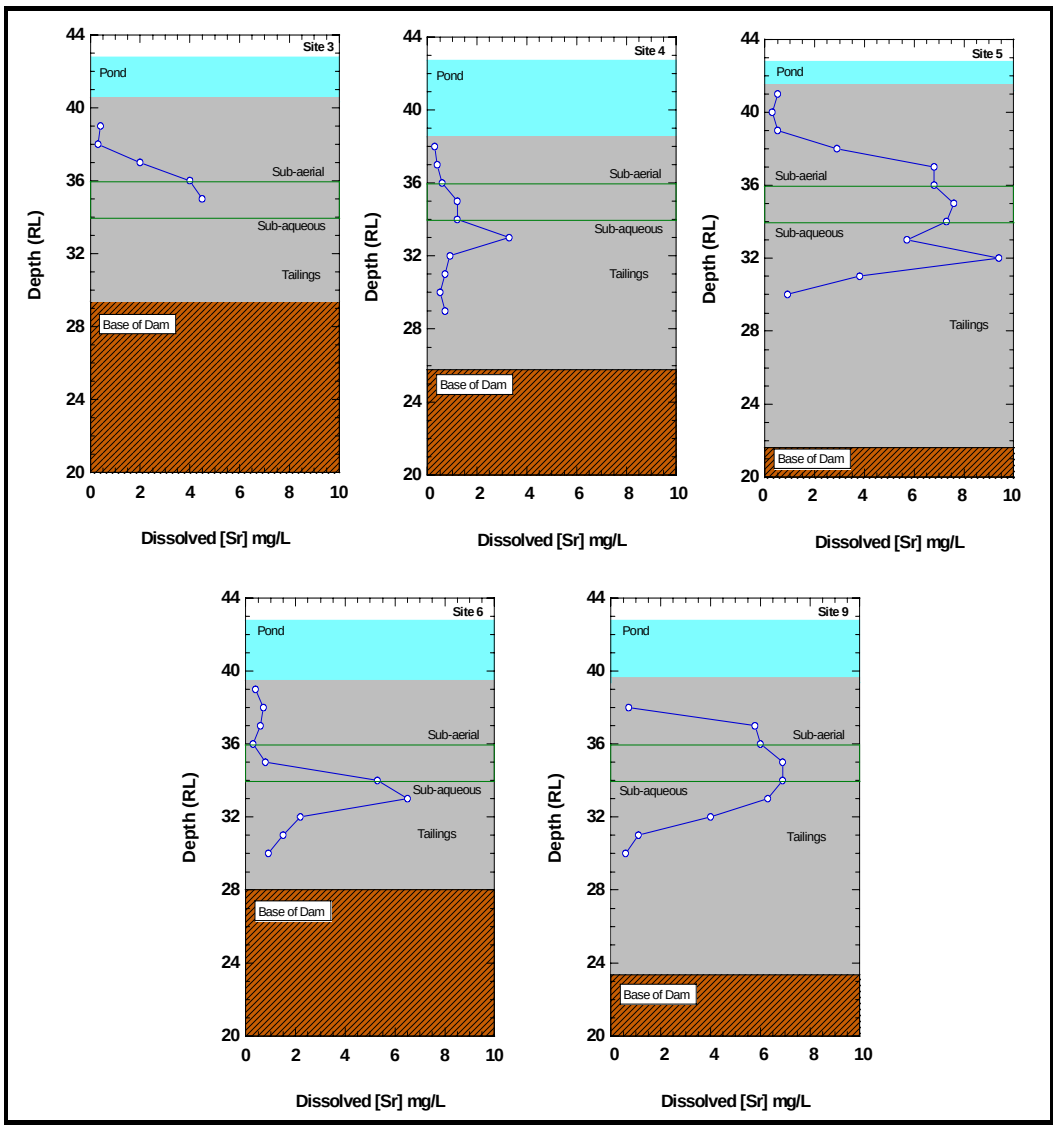

Figure 5.54: Porewater strontium profiles (all stations) – Pond water data were not available at the time of sampling

The results of the solid state speciation test work (Section 5.3.2) support the observed porewater trends in that only a very small percentage (≈7%) of the available Ra was extracted with the alkaline earth phases. In contrast, around 35 to 40% of the available Ra in the gel/fine grain tailings fractions was extracted with the readily reducible Fe and Mn oxyhydroxides (refer to Figure 5.28). This suggests that adsorption processes are controlling the mobility of Ra. Further evidence in support of this notion stems from the fact that Ra activity maxima are generally coincident with elevated levels of dissolved Fe at RL 36 to 40 m (Figure 5.44). This implies that the reductive dissolution of Fe(III) oxides results in the simultaneous release and remobilisation of Ra. Once mobilised and in the presence of excess sulfate (refer to Figure 5.37) it is conceivable that Ra will preferentially co-precipitate with Ba to form sparingly soluble radiobarite [$(Ra,Ba)SO_4$].

Indeed, quantification of saturation indices (SI) using the geochemical speciation program HARPHRQ (Brown et al. 1991) predicts the precipitation of barite under the prevailing geochemical conditions (Table 5.8). Complete details of HARPHRQ and the geochemical model for the tailings pile are provided in Chapter 7.

Table 5.8: Porewater saturation indices for gypsum, celestite and barite at Sites 4 and 9

Site	RL (m)	Gypsum	Celestine	Barite
Site 4	37.6	0.2006	-1.12	0.6111
	36.4	0.1184	-1.18	1.6962
	34.0	0.1680	-1.15	0.9568
	31.7	0.0005	-1.20	0.7571
	29.3	0.0050	-1.21	0.1864
Site 9	38.3	0.1620	-1.24	0.5893
	36.1	0.1471	-1.19	0.5438
	33.8	0.2006	-1.18	0.6546
	31.5	0.0273	-1.20	0.2881
	30.3	0.0404	-1.21	0.2174
Pure Crystalline Barite				0

Saturation indices for both gypsum and barite show a sharp decrease with depth, which suggests that microbial SO_4 reduction is occurring below the zone of Fe oxide reduction. Compared to the SI for pure crystalline barite (McManus et al. 1998), the calculated or apparent porewater SI values are higher indicating that the Ba - host phase differs from the predicted form. Martin et al. (2003) suggested that the discrepancy between the predicted and apparent SI values is explained by either the formation of amorphous barite or some impure form containing Sr. For this study, the former mechanism best explains the observed trends as the SEM-EDX of barite in the tailings did not detect the presence of Sr however it did identify the presence of poorly ordered to microcrystalline barite phases (see Figure 5.17). Porewater Sr concentrations are undersaturated with respect to celestine ($SrSO_4$) indicating that this mineral is unlikely to be influencing the solubility of Ra. However the formation of radiostrontianite ($(Sr, Ra)CO_3$) cannot be ruled out as a possible controlling phase for dissolved Ra in porewaters. This mechanism is further examined in Chapters 6 and 7.

If the apparent SI range of ≈ 0.5 to 1.7 is adopted over the predicted values, it can be assumed that porewaters in the upper tailings zone (above RL 36 m) are saturated with respect to the

poorly ordered barite phase. Furthermore, the levels of sulfate are sufficiently high to maintain saturation, thus inhibiting Ra mobility.

Conversely, porewaters below RL 32 m are possibly undersaturated with respect to the poorly ordered barite phase and thus there is potential for Ra remobilisation. The observed porewater profiles do not show an increase in Ra activity below RL 32, indicating that other geochemical mechanisms are inhibiting mobility. The mechanisms responsible for this anomalous result cannot be elucidated from the available porewater data. However, the controlled conditions of the kinetic column experiments do provide a greater insight into the development of anoxic tailings and the impacts on radium geochemistry.